Structures 29 (2021) 1734–1747

Contents lists available at ScienceDirect

Structures

journal homepage: www.elsevier.com/locate/structures

A machine learning-based formulation for predicting shear capacity of squat flanged RC walls

Duy-Duan Nguyen [a,b], Viet-Linh Tran [b], Dong-Ho Ha [a], Van-Quang Nguyen [b], Tae-Hyung Lee [a,*]

[a] Department of Civil and Environmental Engineering, Konkuk University, Seoul 05029, South Korea
[b] Department of Civil Engineering, Vinh University, Vinh 461010, Viet Nam

ARTICLE INFO

Keywords:
Squat flanged reinforced concrete wall
Shear strength
Artificial neural network
Predictive formula
Graphical user interface

ABSTRACT

The squat flanged reinforced concrete (RC) walls have been widely utilized in nuclear power plant and building structures. Nevertheless, the empirical equations in current design codes and published studies show a significant discrepancy in calculating the shear strength of the walls. The purpose of this study is to develop an effective machine learning model, namely artificial neural network (ANN), for predicting the shear strength of squat flanged RC walls. A total of 369 test results of squat flanged RC walls were collected from the literature and used to develop the ANN model. The results of the proposed model were compared with those of existing design codes and published studies. The comparisons emphasized that the developed ANN model in this paper can predict the shear capacity of squat flanged RC walls more accurately than the existing equations. Moreover, the effect of input parameters on the predicted shear capacity of the walls was sufficiently investigated. A predictive formula based on the ANN model, which can cover thirteen input parameters, was then proposed to compute the shear strength of the squat flanged walls. Additionally, an efficient graphical user interface (GUI) platform has been established for facilitating the practical design process of the squat flanged RC walls.

1. Introduction

Squat or low aspect ratio RC walls have been commonly used in buildings and nuclear power plants since it contributes a significant resistance to the lateral loading capacity of the structures [1]. There are two typical types of cross-sectional shapes of squat RC walls, which are rectangular and flanged sections. For the last few decades, numerous studies have proposed empirical formulas to estimate the shear strength of rectangular RC walls [2–7]. Design codes have already provided calculation guidelines for the rectangular walls [8–10]. However, a practical procedure for computing the shear strength of flanged walls is very limited in existing building codes [11,12]. Additionally, a substantial scattering and biased estimation were produced when the equations in design codes are used to compute the shear capacity of flanged RC walls [1,13–15]. This deviation is obviously due to the presence of flanged boundary elements. Thus, it is necessary to develop a specific formula for estimating the shear strength of such RC walls.

To deal with this problem, some researchers, Gulec and Whittaker [5], Kassem [6], Adorno-Bonilla [7], and Ma et al. [15], have recently proposed empirical formulas to compute the shear strength of squat flanged RC walls. The accuracy of predictive shear strengths based on these models was improved from the design codes. Nevertheless, the equation of Gulec and Whittaker [5] was only limited to squat flanged walls with aspect ratios equal to or less than one. The closed-form formula of Kassem [6], based on the strut-and-tie model, excluded the influence of flange elements, and a large scatter still existed in this model. Even though the predictive strength equations in the studies of Adorno-Bonilla [7] and Ma et al. [15] found to be enhanced, however, the number of databases used was relatively small with 137 and 119 test results, respectively, and the aspect ratios of used test data were mostly less than 1.20. These deficiencies may lead to an inaccurate estimation of the shear strength of squat flanged RC walls. In addition, since these investigations mostly focused on few significant parameters, their predictions were not optimal.

Due to various uncertainties in material properties and configurations, it is challenging to propose a precise empirical model for estimating the shear strength of RC walls. Parameters defining the design equations are generally obtained by performing several tests, but such tests are costly as well as time-consuming. As a surrogate solution, machine learning (ML) paradigms can be used to predict experimental results. The most significant advantage of ML paradigms is certainly dealing with nonlinear problems, which are not easily expressed in

* Corresponding author.
E-mail address: thlee@konkuk.ac.kr (T.-H. Lee).

https://doi.org/10.1016/j.istruc.2020.12.054
Received 19 August 2020; Received in revised form 1 December 2020; Accepted 16 December 2020

Table 1
Formulas for calculating the shear strength of squat flanged RC walls.

No.	Reference	Equation
1	ACI 318–14-Chapter 11 [8]	$V_{n1} = V_c + V_s \leqslant 0.83\sqrt{f'_c} t_w d,\ d = 0.8 l_w$ $V_c = 0.27\lambda\sqrt{f'_c} t_w d + \frac{Pd}{4l_w}$ or $V_c = \left[0.05\lambda\sqrt{f'_c} + \frac{l_w\left(0.1\lambda\sqrt{f'_c} + 0.2\frac{P}{l_w t_w}\right)}{\frac{M}{V} - \frac{l_w}{2}}\right] t_w d$ $V_s = \frac{A_v f_y d}{s}$
2	ACI 318–14-Chapter 18 [8]	$V_{n2} = A_{cv}\left(\alpha_c \lambda \sqrt{f'_c} + \rho_h f_y\right) \leqslant 0.83 A_{cw}\sqrt{f'_c}$
3	ASCE 43–05 [9]	$V_{n3} = \nu_n d t_w,\ (d = 0.6 l_w)$ $\nu_n = 0.69\sqrt{f'_c} - 0.28\sqrt{f'_c}\left(\frac{h_w}{l_w} - 0.5\right) + \frac{P}{4 l_w t_w} + \rho_{se} f_y \leqslant 1.67\sqrt{f'_c}$ $\rho_{se} = A\rho_v + B\rho_h$ if $h_w/l_w < 0.5$ $A = 1$ and $B = 0$ if $0.5 < h_w/l_w < 1.5$ $A = -h_w/l_w + 1.5$ and $B = h_w/l_w - 0.5$ if $h_w/l_w \geqslant 1.5$ $A = 0$ and $B = 1$
4	Wood [3]	$0.5 A_{cv}\sqrt{f'_c} \leqslant V_{n4} = \frac{A_{vf} f_y}{4} \leqslant 0.83 A_{cv}\sqrt{f'_c}$
5	Barda et al. [2]	$V_{n5} = \left(0.67\sqrt{f'_c} - 0.21\sqrt{f'_c}\ \frac{h_w}{l_w} + \frac{P}{4 l_w t_w} + \rho_v f_y\right) t_w d$ $(d = 0.6 l_w)$
6	Gulec and Whittaker [5]	$V_{n6} = \frac{0.04 f'_c A_{eff} + 0.4 F_{vw} + 0.15 F_{vbe} + 0.35P}{\sqrt{h_w/l_w}} \leqslant 15 A_t \sqrt{f'_c}$ (for $h_w/l_w \leqslant 0.1$)
7	Adorno-Bonilla [7]	$V_{n7} = \left(0.54 + 0.19 f'_c - 0.17 f'_c \frac{h_w}{l_w} + 0.45\frac{P}{A_g} + 0.39\rho_{se} f_{yse} + 0.31\rho_{be} f_{ybe}\right) A_{cv}$ $f_{yse} = A f_{yv} + B f_{yh}$ $\rho_{se} = A\rho_v + B\rho_h$ $\rho_{be} = A_{sbe}/A_{cv}$ if $h_w/l_w \leqslant 0.5$ $A = 1$ and $B = 0$ if $0.5 < h_w/l_w < 1.5$ $A = -h_w/l + 1.5$ and $B = h_w/l - 0.5$ if $h_w/l_w \geqslant 1.5$ $A = 0$ and $B = 1$
8	Ma et al. [15]	$V_{n8} = \left(0.32 f_{yf}\rho_f t_f l_f + 0.18 f_{yv}\rho_v t_w z_w + \frac{P}{2}\right)\frac{d_w}{h_w} + 0.54 f_{yh}\rho_h t_w h_w \leqslant 1.4 A_t \sqrt{f'_c}$ $d_w = l_w - t_f - 0.5\left(\frac{0.32 f_{yf}\rho_f t_f l_f + P}{0.59 f'_c t_w} - \frac{t_f l_f}{t_w}\right)$

mathematical models considering the involving variables [16]. The artificial neural networks (ANNs)-based data-driven model, one of the powerful methods in ML, has been widely applied for various engineering problems. This soft computing technique was initially proposed by Ghaboussi et al. [17] and has demonstrated to be capable of modeling the behavior of structures [18–29].

Recently, several studies have employed ML algorithms to predict the shear capacity [30,31] as well as failure mode [32] of RC walls. Chen et al. [30] used the hybrid model, ANN-PSO, to predict the shear strength of squat rectangular RC walls based on a collection of 139 test results. They concluded that the proposed model predicted the strength of shear walls more accurately than other models. However, an application of such hybrid model to engineering designs is unfeasible since a mathematically practical formula was not provided. Also, a predictive model for the flanged RC wall type was not established in their work. Moradi and Hariri-Ardebili [31] constructed a library of shear-wall database and then developed an ANN model for estimating shear strength of generic RC walls. In this database, they included both slender and squat walls as well as rectangular and flanged cross-section types. While their results demonstrated the accuracy of the ANN model, the scattering of the testing and validation was still large, and unfortunately, a practical equation or a GUI tool for the design process was not provided.

The purpose of this study is to develop an efficient ANN-based data-driven model to predict the shear strength of squat flanged RC walls, which are critical structural members, particularly, in nuclear power plants. A set of 369 experimental tests of squat flanged RC walls were carefully collected to develop the machine learning model. The results of the proposed model were compared with those of existing design codes and published studies. Moreover, the effects of input parameters on the predicted shear capacity of the walls were investigated thoroughly. A predictive formula based on the ANN model considering thirteen input parameters was then proposed to compute the shear strength of flanged walls. Finally, a beneficial GUI tool was also developed for facilitating the practical design process of the squat flanged RC walls.

2. Existing formulas for calculating the strength of RC shear walls

In this study, eight typical formulas to calculate the shear strength of the squat flanged RC walls were reviewed. Those equations were either specified in design codes [8,9] or proposed by various studies [2,3,5,7,15]. Table 1 summarizes the selected equations for obtaining the shear strength of squat flanged RC walls. In this table, the first four equations are used for general shear walls, including slender and squat rectangular RC walls, while the later four equations are specifically applied for squat and flanged RC walls.

The parameters for calculating the shear strength (V_n) of shear walls in Table 1 can be classified into four groups: (1) geometric parameters, (2) material properties, (3) external applied loads and forces attributed by reinforcements, and (4) coefficients. Geometric parameters includes the wall height (h_w), the web length (l_w), the web thickness (t_w), the flange length (l_f), and the flange thickness (t_f), the gross area of concrete section bounded by web thickness and length of the section in the direction of shear force (A_{cv}), the area of wall without flanges (A_t), the effective area for flanged walls (A_{eff}), and the area of vertical

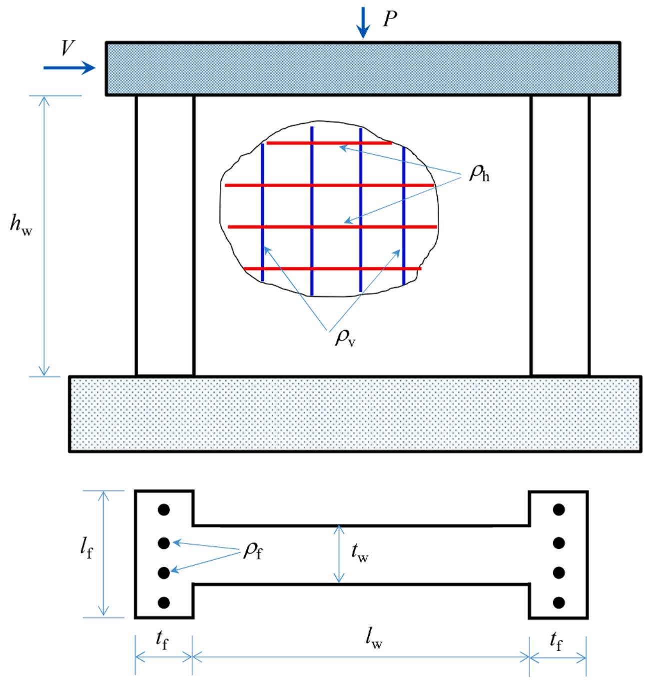

Fig. 1. Illustration of squat flanged RC walls.

reinforcements in one boundary element (A_{sbe}). Material properties consist of the compressive strength of concrete (f'_c), the yield strength of the horizontal (f_{yh}) and vertical (f_{yv}) reinforcements, the reinforcement ratios of the walls in the horizontal (ρ_h) and vertical (ρ_v) directions, the longitudinal reinforcement ratios of the flanged element (ρ_f). External loads are the lateral (V) and axial force (P), while the forces attributed by reinforcements in vertical web, horizontal web, and vertical boundary elements (i.e. flanges) are F_{vw}, F_{hw}, and F_{vbe}, respectively. The coefficients are the one defining the relative contribution of concrete strength to nominal wall shear strength (α_c) and the modification factor (in ACI 318–14) reflecting the reduced mechanical properties of lightweight concrete relative to normal weight concrete of the same compressive strength (λ).

3. Experimental database

To develop the ANN model, a total of 369 experimental data of squat flanged RC walls were collected from the literature [2,11,33–62]. Thirteen important input parameters are required to estimate the shear strength of the walls including the geometric and material properties. Geometric parameters of the wall are the height (h_w), the web length (l_w), the web thickness (t_w), while the dimensions of flange elements are the length (l_f) and thickness (t_f), as shown in Fig. 1. It was shown that the aspect ratio (h_w/l_w) of the tested walls was equal to or less than 2.0, which obviously confirmed to the squat wall classification. In the database, the compressive strength of concrete (f'_c) ranged from 12 to 93 MPa, while the yield strength of the horizontal (f_{yh}) and vertical (f_{yv}) reinforcing bars of RC walls varied from 224 to 792 MPa. The reinforcement ratios of the walls in the horizontal (ρ_h) and vertical (ρ_v) directions ranged from 0.1% to 2.9%, while the longitudinal reinforcement ratios of the flanged element (ρ_f) ranged from 0.1% to 6.4%. A variation of the axial load (P) from 0 to 2,364 kN was considered in the database. The statistical properties of the test results are presented in Table 2. It should be noted that *SD* and *COV* were the abbreviations of the standard deviation and the coefficient of variation, respectively. Fig. 2 shows the histograms of thirteen input parameters based on the 369 selected experimental data.

4. ANN model for shear strength of flanged RC walls

4.1. ANN architecture

Recently, the ANNs model has emerged as a powerful and versatile computational tool for organizing and correlating knowledge [63]. The multi-layer feed forward perceptron (MLP), depending on the error back-propagation, is the most popular of the feed-forward neural network, was employed to train the data in this study [64]. An MLP algorithm comprises of neurons, which are classified into three components: (1) input layer, which allows to enter input parameters, (2) one or more hidden layers, and (3) an output layer, which contains the predicted result. These neurons are connected in some way, in which the connection holds a weight, and each neuron contains a bias and an activation. Assuming that the input vector of the neuron is $x = [x_1, x_2, \cdots, x_m]$ and the weighted sum of the input signals is expressed by $z \in R$:

$$z = \sum_{i=1}^{d} w_i x_i = w^T x + b \tag{1}$$

where $w = [w_1, w_2, \cdots, w_d] \in R^d$ is the weight vector of d dimensions and $b \in R$ is the bias. It is required to perform nonlinear processing on z to represent the nonlinear relation between input and output layers, expressed by

$$y = f(z) \tag{2}$$

where f denotes the activation function, while y represents the activation value of the neuron.

Obviously, the activation function is the crucial element for providing a smooth and differentiable transition during training of the network. For this study, the *tansig* and *purelin* functions were used according to the recommendation of Nikbin et al. [65], expressed as follows.

$$y = tansig(x) = \frac{2}{1 + e^{-2x}} - 1 \tag{3}$$

$$y = purelin(x) = x \tag{4}$$

It should be noted that the *tansig* function just scales the output to be between −1 and 1, meanwhile, the *purelin* function generates the output from $-\infty$ to $+\infty$, as shown in Fig. 3.

The feed-forward back-propagation algorithm includes two processes: (1) feed-forward or forward pass and (2) back-propagation or backward pass. For the forward pass, the input data are provided to the

Table 2
Statistical characteristics of input parameters of collected experiments.

Input parameter	h_w(mm)	l_w(mm)	t_w(mm)	t_f(mm)	l_f(mm)	ρ_f(%)	ρ_v(%)	ρ_h(%)	f'_c(MPa)	f_{yf}(MPa)	f_{yv}(MPa)	f_{yh}(MPa)	P(kN)	V_n(kN)
(Variable)	(X1)	(X2)	(X3)	(X4)	(X5)	(X6)	(X7)	(X8)	(X9)	(X10)	(X11)	(X12)	(X13)	(Output)
Min	400	507	10	60	60	0.07	0.07	0.00	12.3	208.9	224.1	224.1	0.0	34.32
Mean	1051	1542	82	176	238	1.5	0.8	0.8	31.1	385.1	397.6	396.3	325.4	678.53
Max	2200	3960	160	600	1500	6.4	2.9	2.8	93	1009	792	792	2364	2511.0
SD	465	664	37	98	264	1.3	0.6	0.6	13.3	87.4	82.7	81.5	485.2	602.02
COV	0.44	0.43	0.45	0.56	1.11	0.87	0.75	0.73	0.43	0.23	0.21	0.21	1.59	0.887

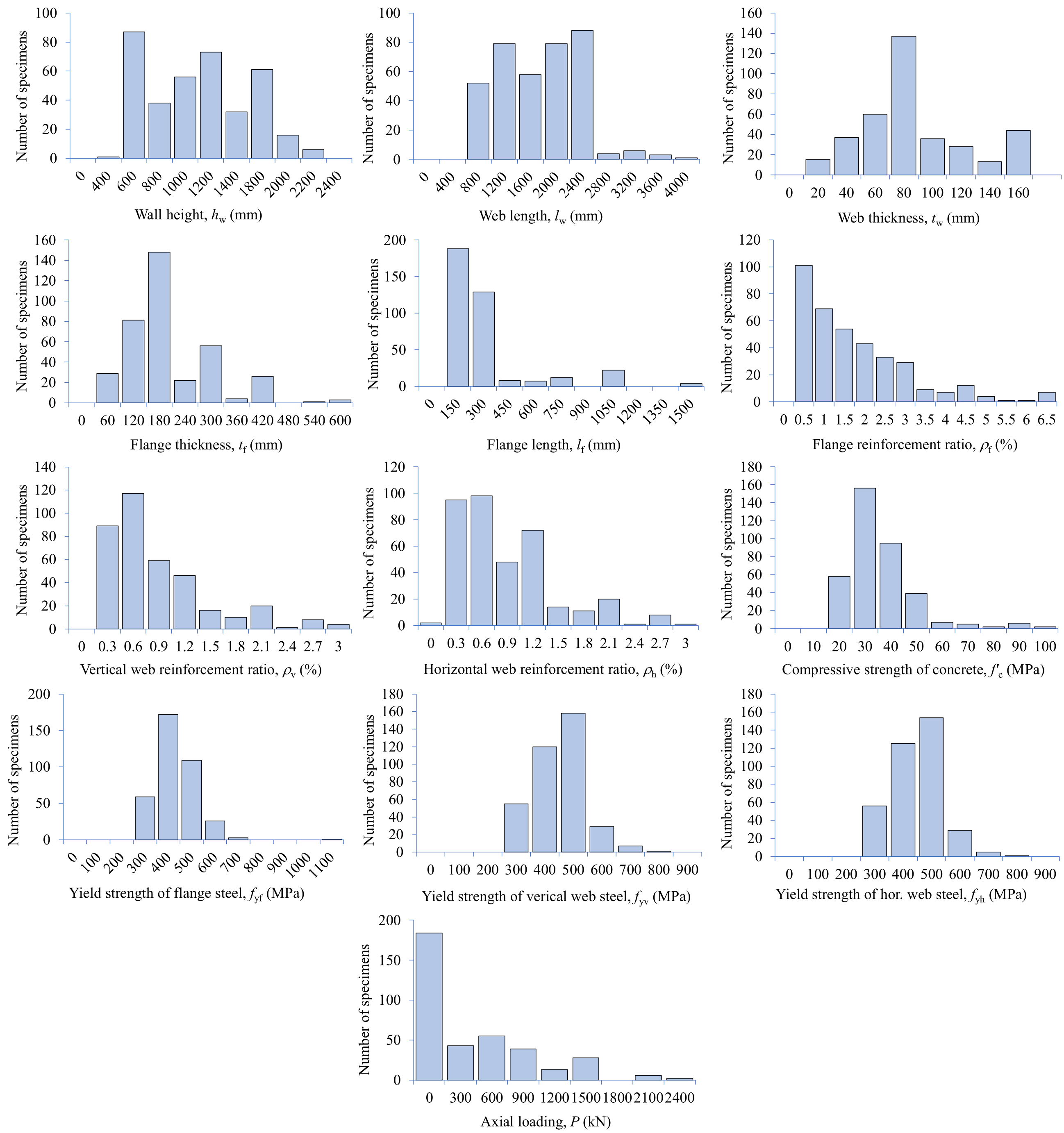

Fig. 2. Histograms of input parameters based on 369 experimental data.

input layer, which transfers the information forward, through the different connections, from one neuron to another in the network. Since the output from forward pass is obtained, the next step is to assess this output by comparing it with the target using the mean squared error (*MSE*). To find the optimal weights and biases that can minimize the *MSE*, i.e. the backward pass process, it is needed to quantify the error produced by each of weights and biases, and iteratively update them until the *MSE* is converged. The *MSE* is expressed as

$$MSE = \frac{1}{N}\sum_{i=1}^{N}(p_i - t_i)^2 \tag{5}$$

where N is the number of samples; t_i and p_i are the target and predicted values of the i^{th} sample, respectively.

The over-fitting problem, a deficiency in machine learning, refers to a model that training too well, and it therefore hinders the accuracy and performance of the model on new data. To prevent over-fitting, some typical solutions can be used such as cross-validation, training with more data, removing features, and regularization. In this study, the regularization technique was applied for modifying the error function as a summation of *MSE* and the mean squared network weights and biases, expressed as follows.

$$MSEREG = \gamma MSE + (1-\gamma)MSWB \tag{6}$$

where γ is the performance ratio and *MSWB* is the mean squared network weights and biases, which is calculated by

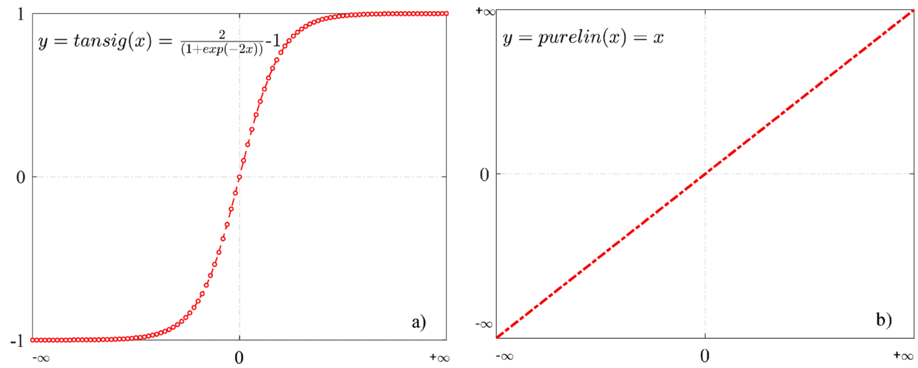

Fig. 3. Activation functions of ANN model: (a) *tansig* and (b) *purelin* function.

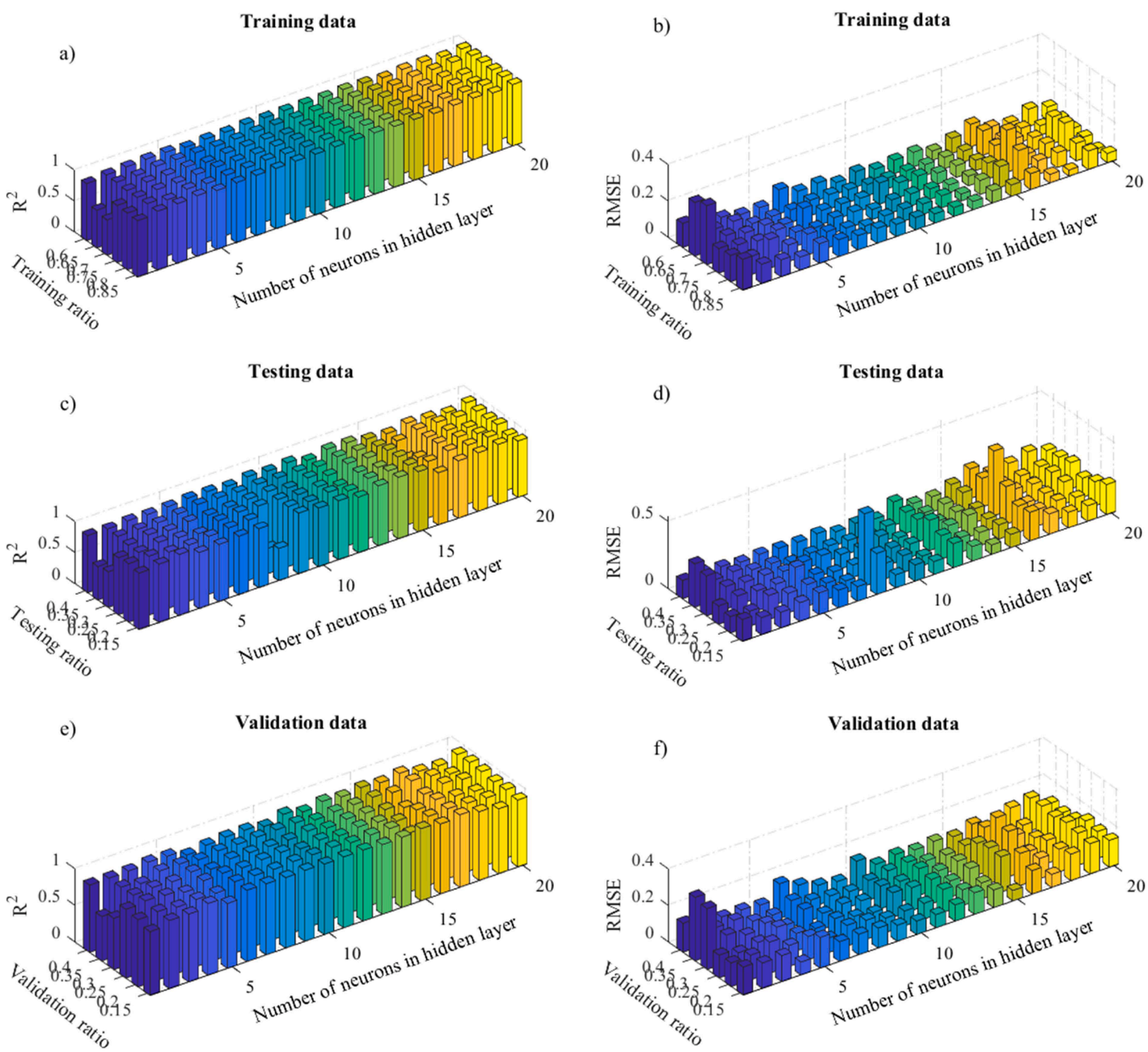

Fig. 4. Performance of different ANN models.

$$MSWB = \frac{1}{N}\sum_{j=1}^{N}\varpi_j^2 \tag{7}$$

Furthermore, to enhance the accuracy of the ANN models and to avoid unexpected errors during the training and testing process, the database is normalized within the range of −1 and 1 using the following expression

$$X_n = 2 \times \frac{X - X_{min}}{X_{max} - X_{min}} - 1, \tag{8}$$

where X is the data sample, X_n is the normalized data sample, $X_{\min}$ and $X_{\max}$ are the minimum and maximum values of considered parameters,

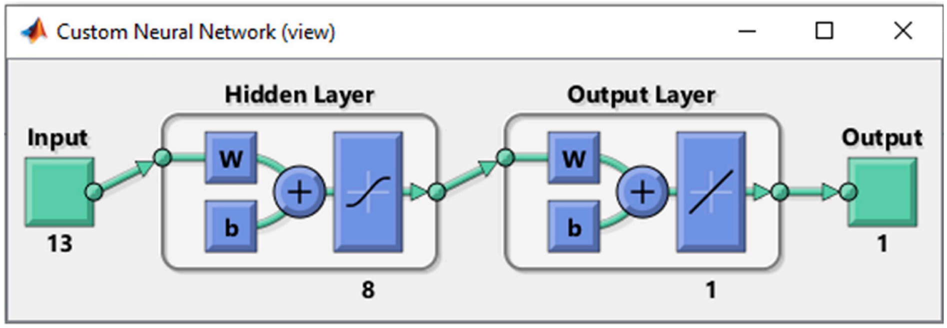

(a) Illustrative architecture of the ANN model

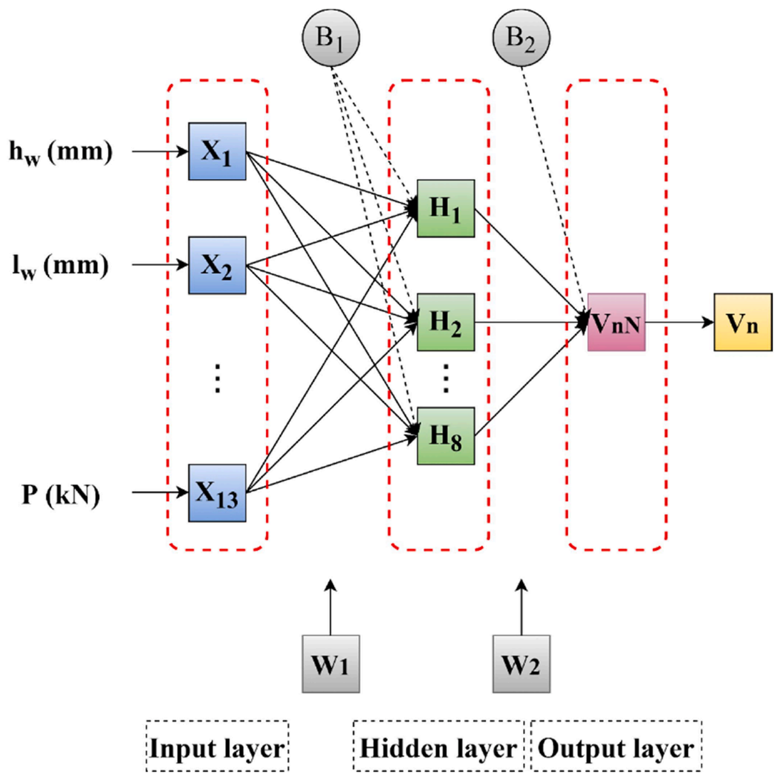

(b) Detailed structure of the ANN model

Fig. 5. Depiction of the proposed ANN model.

respectively.

To optimize the performance of an ANN model, a good architecture of the ANN model should be determined. In this study, the trial and error method was used to obtain the number of hidden layers as well as the number of neurons in each hidden layer. We tried with various architectures, in which the training ratio changed from 0.6 to 0.85 and the number of hidden layers varied from 1 to 20. The Levenberg-Marquardt algorithm, one of the fastest back-propagation algorithms in training, was used to tune the weights and biases of ANN models [66]. This algorithm was consistent with studies elsewhere [25,28]. Two statistical indicators, the coefficient of determination (R^2) and root mean square error (*RMSE*), were obtained to demonstrate the performance of the ANN models. Fig. 4 shows a series of the recorded values of R^2 and *RMSE* based on the trial and error process. Finally, the best ANN architecture with the highest value of R^2 and the lowest value of *RMSE* in training, testing, and validating phase was chosen. This ANN model comprises the training ratio of 0.75, the testing and validating ratios of 0.125, and 8 neurons in the hidden layer.

Fig. 5 depicts the developed ANN model, in which the number of neurons is decided by the input and output parameters considered. Herein, 13 neurons in the input layer represent the 13 input parameters as listed in Table 2, and one neuron in the output layer was for the peak shear strength of the walls (V_n). Eight neurons in the hidden layer were determined using the sensitivity analysis, which provided the best performance of the model. It should be noted that the developed ANN model was implemented using MATLAB [67].

4.2. Performance of the proposed ANN model

Fig. 6 shows the performance of the developed ANN model, in which MSEs for the training, validation, and testing decrease as the epoch increases. The best validation performance is determined as the *MSE* of 6.1545×10^{-3} at the 8^{th} epoch, which implies that the ANN model was trained well.

Fig. 7 shows the comparison between the predicted results of the ANN model and experimental data. It can be found that the results obtained from the ANN model were well matched with experiments for both training, testing, and validation. In other words, the developed

Structures 29 (2021) 1734–1747

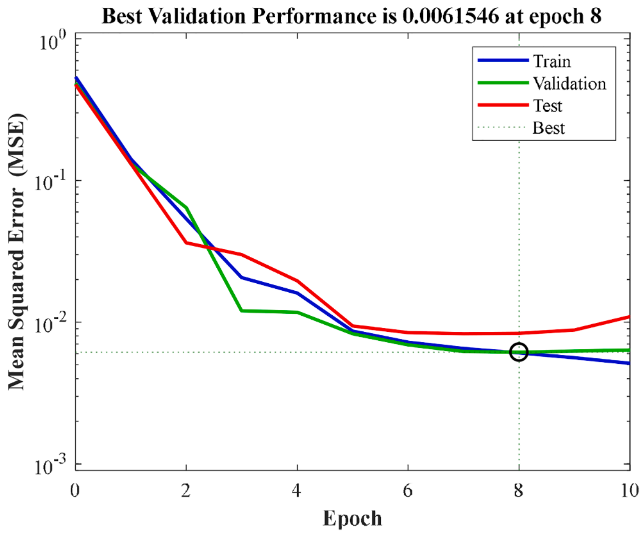

Fig. 6. Performance of the ANN model.

ANN model demonstrated good performance and it was highly reliable in estimating the shear strength of the squat flanged RC walls.

5. Comparison between the proposed ANN model and existing results

5.1. Validation criteria

In this study, three indicators, which are coefficient of determination (R^2), root square error (*RMSE*), and $a20-index$, were employed to assess the performance of different predictive models. Those indicators are expressed in following equations.

$$R^2 = 1 - \frac{\sum_{i=1}^{n}(t_i - o_i)^2}{\sum_{i=1}^{n} o_i^2}, \tag{9}$$

$$RMSE = \sqrt{\frac{1}{n}\sum_{i=1}^{n}(t_i - o_i)^2}, \tag{10}$$

$$a20-index = \frac{m20}{M}, \tag{11}$$

where t_i and o_i are the target and output of i^{th} sample, respectively; n is the number of samples, M is the number of the data sample and $m20$ is the number of samples with the value of the ratio of experimental value to a predicted value falling between 0.80 and 1.20.

The value of R^2 was used to measure the variation between predicted and experimental data. Meanwhile, the *RMSE* value represents the mean of errors. Moreover, the $a20-index$ is an useful statistical property,

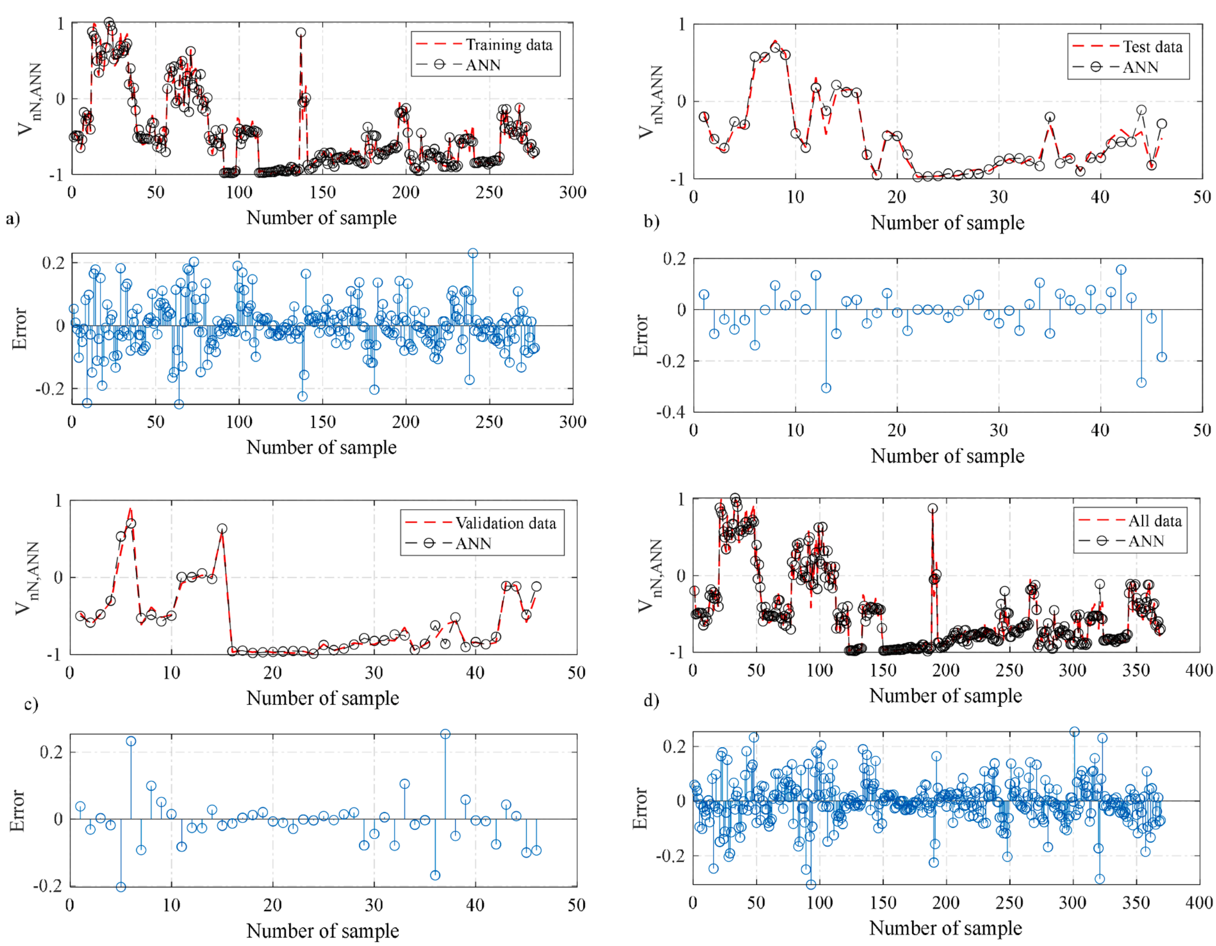

Fig. 7. Comparison with experimental results.

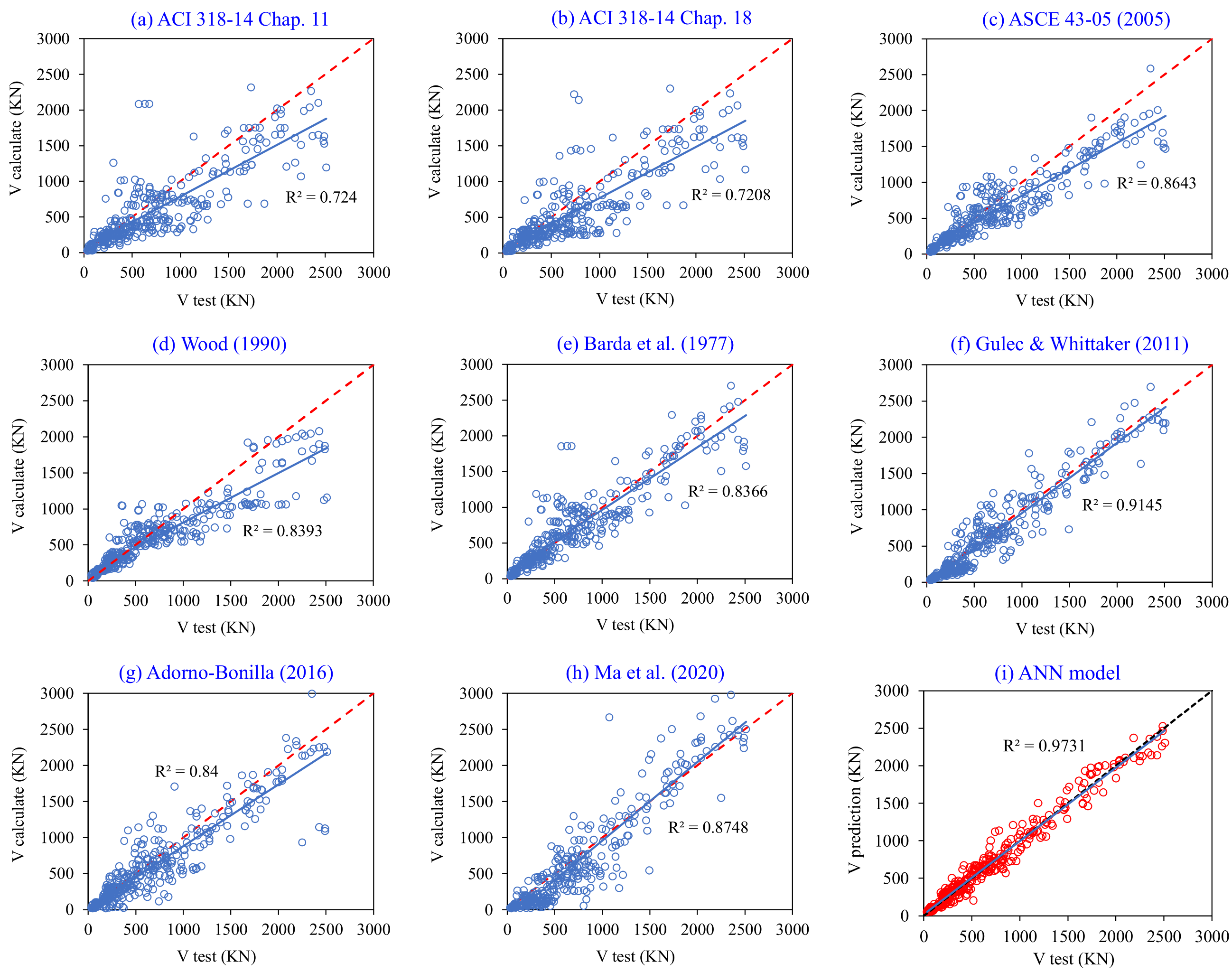

Fig. 8. Comparisons of shear strength between test results and different calculated methods.

which represents the number of predicted data falling in a deviation of ± 20% compared with experimental data [68,69]. Generally, the higher value of R^2 and the lower value of *RMSE* indicate a good performance of the model. For a perfect predictive model, the value of $a20-index$ is expected to be 1.0.

5.2. Results and discussions

Fig. 8(a-h) shows the comparisons of predicted peak shear strengths of existing models and experimental results. The dashed line (i.e. the 1:1 line) indicates target values, while the solid line represents the linear regression of the scatters. The closer scattering to the 1:1 line, the higher accuracy of the predicted result. It can be observed that the shear strengths calculated from ACI 318–14 [8], ASCE 43–05 [9], and Wood [3] were mostly lower than the test results. This underestimation can be attributed to those equations that were sorely proposed for rectangular RC walls and the influence of flanges was neglected. On the other hand, the mean calculated results from equations of Barda et al. [2], Gulec and Whittaker [5], Adorno-Bonilla [7], and Ma et al. [15] were close to the experiments. Considering the flange elements in the predictive equations, these models have improved the accuracy of estimation. Among that, the equations of Gulec and Whittaker [5] and Ma et al. [15] demonstrated a good prediction with a higher R^2 value, and the linear regression was relatively matched with the 1:1 line.

The predicted results obtained from the ANN model are also compared with the experimental data, as shown in Fig. 8(i). It was found that the scattering of the proposed ANN model in this study was significantly smaller compared with those of previous models. Moreover, the linear regression line of the plotting data was mostly identical to the diagonal line with a high R^2 value of 0.973. Fig. 9 shows the histograms of the proposed ANN model, indicating a good distribution with the mean value of unity.

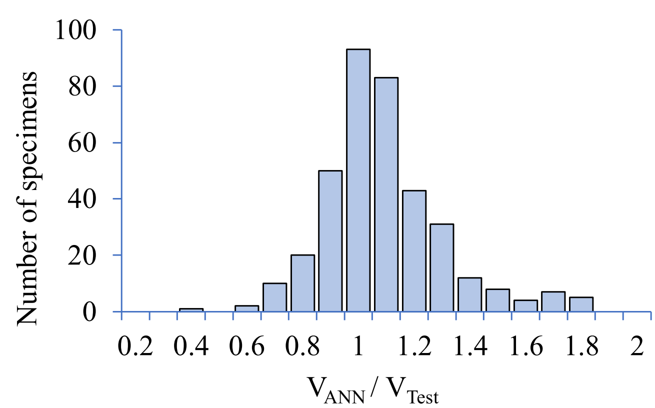

Fig. 9. Histograms of proposed ANN model.

Fig. 10 shows the box plot of predicted-to-tested strength ratios with different predictive models and Table 3 presents the statistical properties of predicted-to-tested strength ratios in various models. It

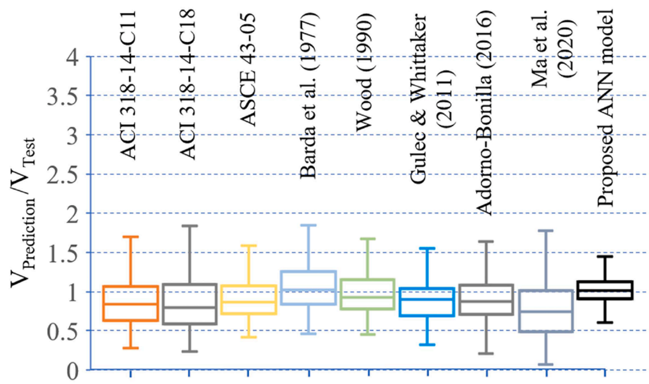

Fig. 10. Box plot of predicted-to-tested strength ratios of squat flanged RC walls.

highlighted that the ANN model is capable of estimating shear strength of squat flanged RC walls with the highest accuracy in terms of the lowest COV and SD as well as the mean value close to unity. It is again to show that the R^2 value of the proposed ANN model was the largest among considered models. Similar to the R^2 value, the $a20-index$ of the ANN model (i.e. 0.73) showed to be superior to that of other models. Also, the *RMSE*, which represents the error between prediction and target (i.e. experiment) values, was smallest for the ANN model, followed by Gulec and Whittaker [5] and Barda et al. [2]. Furthermore, the SD and COV of the ANN model, 0.22 and 0.21 respectively, are considerably smaller than those of other models, and the mean value of 1.04 is very close to 1.0. These implies that the proposed ANN model is highly reliable in estimating the shear strength of the squat flanged RC walls.

6. Parametric study

In this section, a parametric study was performed to identify the effects of input variables on the shear strength of the walls. For that, each input parameter was varied from the minimum to maximum value, which is based on the database in Table 2, while other parameters were set to the mean values. The variation of the output due to the variation of the single input parameter are monitored. However, the effects of multiple variations of different input parameters on the shear strength of RC walls were not investigated in the current study.

6.1. Effect of wall height

Fig. 11 shows the influence of the wall height (i.e. X1) on the strength of squat flanged RC shear walls. The dashed curve with triangular markers represented the variation of the parameter from the lower to the upper bound, while the continuous finger-print curves showed the contour of the variation. It was observed that the increment of the height of walls caused a decrement of calculated shear strength. The strength was gradually reduced more than triple times as the wall height varied from the minimum to maximum. This can be attributed to the fact that the lateral stiffness of the wall was decreased as the aspect ratio increased.

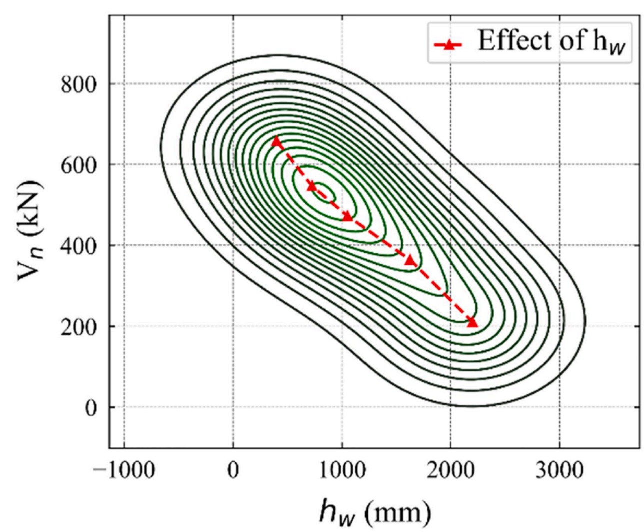

Fig. 11. Effects of the wall height.

6.2. Effect of web dimensions

The dimensions of the web, including the length (i.e. X2) and thickness (i.e. X3) contribute significantly to the shear capacity of RC walls. As shown in Fig. 12, the strength of RC walls is increased with an increment of the web's dimensions. The shear strength was approximately five times increased as the web dimensions ranged from the minimum to the maximum. It was because of the increment of the shear area as the length and thickness enlarged.

6.3. Effect of dimensions of flanges

Fig. 13 shows the effects of the thickness (i.e. X4) and the length (i.e. X5) of flanges on the strength of the wall. The flange dimensions are shown to be the most influential parameters on improving the shear capacity of the squat flanged RC wall. It can be observed that the strength is slightly increased as those parameters varied from the minimum to the mean value. However, it is magnified from the mean to the maximum level of the dimensions of flanges. The strength is increased approximately four times between the range of flange thickness, while it

Table 3
Performance of different models.

No.	Predicted model	R^2	*RMSE* (kN)	*a20-index*	Statistical properties of $V_{Prediction}/V_{Test}$				
					Min	Max	SD	Mean	COV
1	ACI 318–14. C11 [8]	0.724	339	0.39	0.28	4.11	0.48	0.92	0.53
2	ACI 318–14. C18 [8]	0.720	347	0.33	0.24	3.29	0.45	0.89	0.50
3	ASCE 43–05 [9]	0.864	258	0.50	0.41	2.91	0.33	0.93	0.35
4	Wood [3]	0.839	276	0.49	0.45	2.96	0.37	1.01	0.36
5	Barda et al. [2]	0.836	245	0.52	0.46	3.87	0.44	1.11	0.40
6	Gulec and Whittaker [5]	0.914	183	0.50	0.32	2.25	0.31	0.91	0.34
7	Adorno-Bonilla [7]	0.840	251	0.48	0.07	2.62	0.36	0.91	0.40
8	Ma et al. [15]	0.874	265	0.33	0.07	2.48	0.38	0.77	0.49
9	ANN model	0.973	107	0.73	0.39	1.75	0.22	1.04	0.21

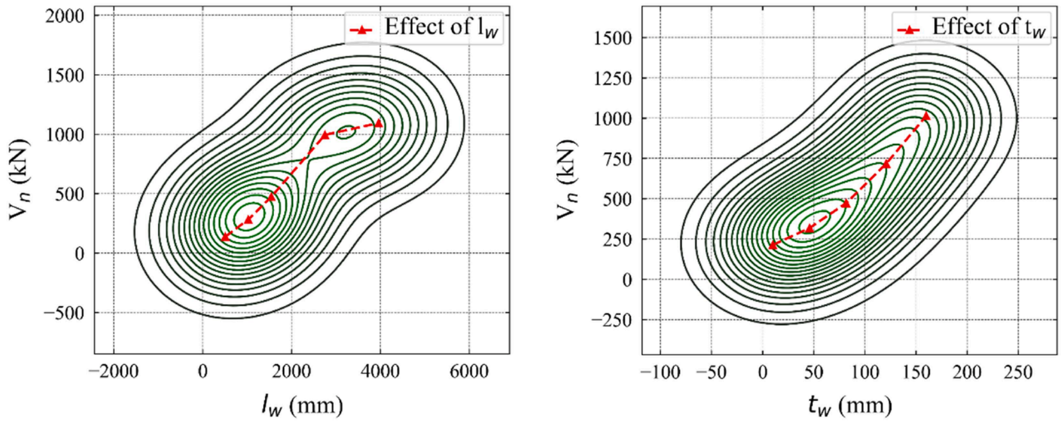

Fig. 12. Effects of web dimensions.

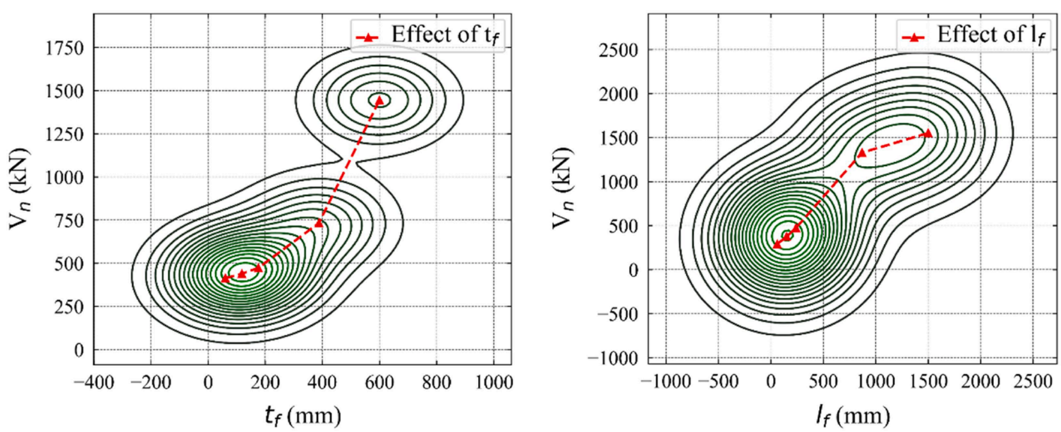

Fig. 13. Effects of flange dimensions.

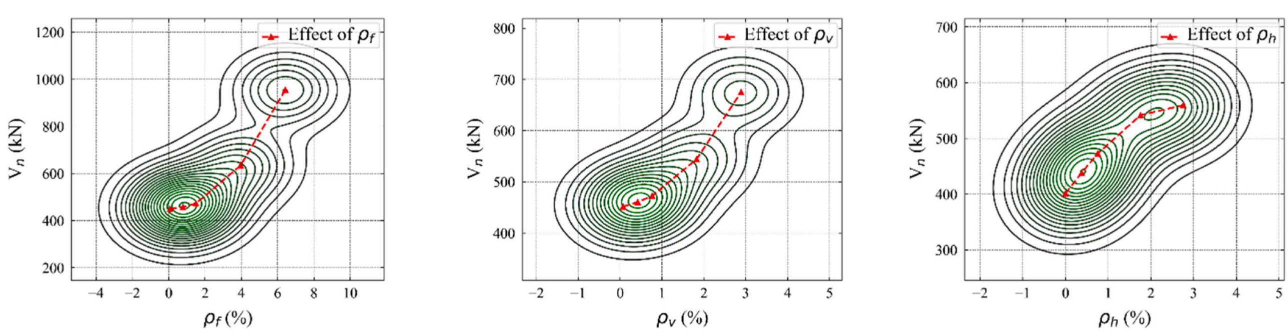

Fig. 14. Effects of reinforcement ratios.

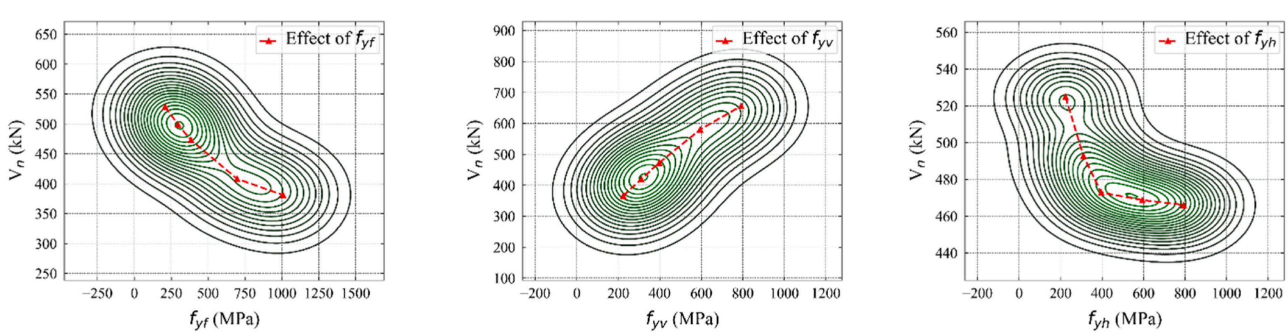

Fig. 15. Effects of the yield strength of reinforcement bars.

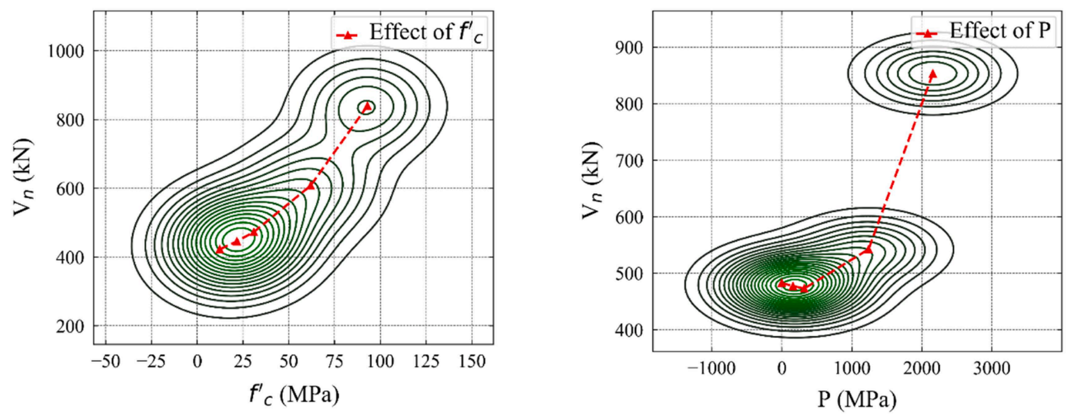

Fig. 16. Effects of the compressive strength of concrete and axial load.

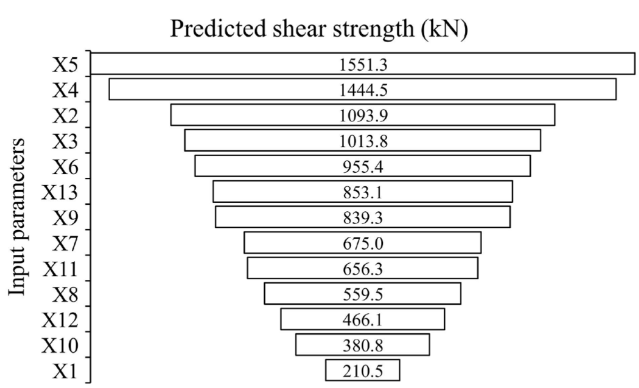

Fig. 17. Sensitivity of input parameters to the shear strength of squat flanged RC walls.

is increased roughly eight times with a variation of the flange length. This observation highlights that the capacity of RC walls can be significantly enhanced by adding the flange elements, which enlarged the shear area of the walls.

6.4. Effect of reinforcement ratio

The influences of reinforcement ratios on the strength of RC walls are shown in Fig. 14. The variations of the vertical (i.e. X7) and horizontal (i.e. X8) reinforcement ratios of the web affected the capacity of the flanged RC walls insignificantly. Meanwhile, the reinforcement ratio of the flange element (i.e. X6) had a moderate effect with a double increment of the shear strength between the lower and the upper limit.

6.5. Effect of yield strength of reinforcing bar

Fig. 15 shows the effects of yield strengths of reinforcing bars on the shear strength of flanged RC walls. The yield strengths of reinforcements of the web and flanges were inefficient at changing the shear strength of the squat flange RC walls. This observation was consistent with the finding of Baek et al. [70].

6.6. Effect of compressive strength of concrete and axial load

Fig. 16 shows the effects of the compressive strength of concrete (i.e. X9) and axial load (i.e. X13) on the shear strength of squat flanged shear walls. These parameters have a moderate influence on the capacity of the walls. It is shown that the strength was slightly increased as X9 and X13 varied from the minimum to the mean level. Once the parameters reached the upper limit, the strength is approximately doubled.

Fig. 17 summarizes the sensitivity of all input parameters in predicting the strength of the squat flanged RC walls. It should be noted that the output in this figure was obtained at the maximum of each input parameter. It is observed that the dimensions of the flange (i.e. X5 and X4) were the most influential parameters on improving the shear capacity of the flanged RC walls, followed by the dimensions of the web. In contrast, the height of the wall (X1) negatively affected the shear strength of the walls. Moreover, the yield strengths of reinforcements of the flange and web (i.e. X10, X11, and X12) and the horizontal reinforcement ratio of the web (X8) have a trivial influence on the strength of the walls.

7. Practical tools for calculating shear strength squat flanged RC walls

7.1. ANN formula

To apply the ANN model for design problems, it is necessary to transform the ANN into an explicit mathematical formula. Based on the proposed ANN model, the formula to estimate the shear strength of squat flanged RC walls was expressed as a nonlinear form in Eq. (12). V_n is the real value of the shear strength. The form of this equation comes from the denormalization procedure of Eq. (8). As a result, the value of 34.3230 is the minimum value of the shear strength of the database. The value of 1238.3 is a half of the difference of maximum and minimum shear strength values of database, as shown in Table 2.

$$V_n = 1238.3 \times (V_{nN} + 1) + 34.3230, \tag{12}$$

where V_{nN} is a normalized shear strength of squat flanged RC walls, expressed by

$$\begin{aligned} V_{nN} = & -1.7394 \times A_1 - 1.1671 \times A_2 - 0.4155 \times A_3 + 1.2467 \times A_4 + 1.5423 \\ & \times A_5 - 0.5019 \times A_6 - 1.2129 A_7 + 1.2618 \times A_8, \end{aligned} \tag{13}$$

where A_1 to A_8 are eight coefficients that represent the hidden neurons' outputs. A *tansig* function was also applied for calculating the A_1 to A_8 coefficients, resulted as

$$
\begin{bmatrix} A1 \\ A2 \\ A3 \\ A4 \\ A5 \\ A6 \\ A7 \\ A8 \end{bmatrix} = TANSIG\left(\left(\begin{bmatrix}
0.691 & 1.2578 & 0.1449 & -0.5425 & -0.5203 & -0.3906 & -0.004 & 0.408 & 0.3379 & 0.2529 & -0.3966 & -0.2438 & -0.1093 \\
0.6907 & 0.9494 & 0.6157 & 0.3965 & -0.164 & -0.155 & 0.6026 & 0.0984 & 0.5386 & -0.3896 & 0.6216 & 0.2388 & 0.1393 \\
0.2765 & -1.4959 & -0.1142 & 0.5818 & 0.2478 & -1.0525 & -0.0239 & -0.1902 & -0.7352 & 0.4445 & 0.014 & -0.6613 & -0.8926 \\
-0.5638 & 1.0797 & 1.0395 & 0.6424 & 1.7571 & -0.2133 & 0.5438 & 0.0673 & 0.2683 & -0.4038 & 0.1597 & -0.5513 & 0.2675 \\
0.3497 & 1.2535 & 0.5886 & 0.0185 & 1.2229 & -0.0079 & -0.2191 & 0.4352 & 0.0819 & 0.2188 & 0.3861 & -0.1022 & -0.7269 \\
-0.6911 & 0.6884 & -1.1609 & -0.9323 & 0.1533 & -0.1017 & -0.5411 & -0.5799 & -0.8492 & -0.8749 & -0.3336 & 0.6164 & 0.7163 \\
-0.7026 & 0.9643 & 0.3298 & 0.1724 & 0.8133 & 0.3941 & -0.6423 & -0.0419 & 0.4143 & -0.0373 & 0.7065 & 1.0827 & -0.518 \\
1.1623 & -0.2146 & 0.2766 & -1.2189 & -0.5556 & 0.4034 & 0.1606 & -0.0196 & -0.2378 & -0.4324 & 0.5005 & -0.2772 & -0.0503
\end{bmatrix}
\begin{bmatrix} X_1^N \\ X_2^N \\ X_3^N \\ X_4^N \\ X_5^N \\ X_6^N \\ X_7^N \\ X_8^N \\ X_9^N \\ X_{10}^N \\ X_{11}^N \\ X_{12}^N \\ X_{13}^N \end{bmatrix}\right)
+ \begin{bmatrix} -0.8612 \\ 0.4836 \\ -0.4291 \\ 0.4410 \\ 0.3008 \\ 0.0339 \\ -0.6922 \\ -0.7685 \end{bmatrix}\right) \tag{14}
$$

It is noted that ANN cannot deal with an extrapolation, therefore the input parameters should be limited within the lower (i.e. minimum) and upper value (i.e. maximum) of the training data. A wide range of collected datasets should be used to enlarge the margin of the ANN model and to enhance the performance as well as reliability of the model.

7.2. GUI tool

If the mathematical formula is still challenging for engineers, a user-friendly software tool can be a favorably alternative option. A practical GUI tool was developed using MATLAB [67] to facilitate the design process for calculating the shear strength of squat flanged RC walls, as shown in Fig. 18. In this tool, 13 input parameters, from X1 to X13, are provided. Also, eight neurons (nodes) in the hidden layer are shown. This tool is free-of-charge and convenient to use, in which it can readily obtain the shear strength by just going to the 'Start Predict' button after entering the input parameters. It takes less than one second to achieve the output result. Note that users can find the GUI tool in the supplemental materials, which are accompanied with this article link. Since the GUI tool is developed using the proposed ANN model, the accuracy of prediction was verified and thoroughly emphasized in the previous section.

8. Conclusions

An efficient machine learning formulation, namely the ANN model, to predict the shear strength of squat flanged RC walls was developed based on a set of 369 experimental results. The results of the proposed model were compared with those of eight existing formulas in design codes and published studies. The following conclusions are drawn.

- The developed ANN model in this study predicts the shear strength of squat flanged RC walls more accurately than the existing equations. The accuracy of the model is verified by the statistical properties of the predicted-to-measured strength ratio including the SD, mean value, COV, R^2 value, *RMSE*, and $a20-index$.
- The most influential parameters on improving the shear strength of flanged RC walls are the length of the web, dimensions of the flanges, and the thickness of the web. Meanwhile, the height of the wall has a contrary effect to the strength capacity of the walls, in other words, the higher wall the lower shear strength obtained. The yield strength of reinforcements

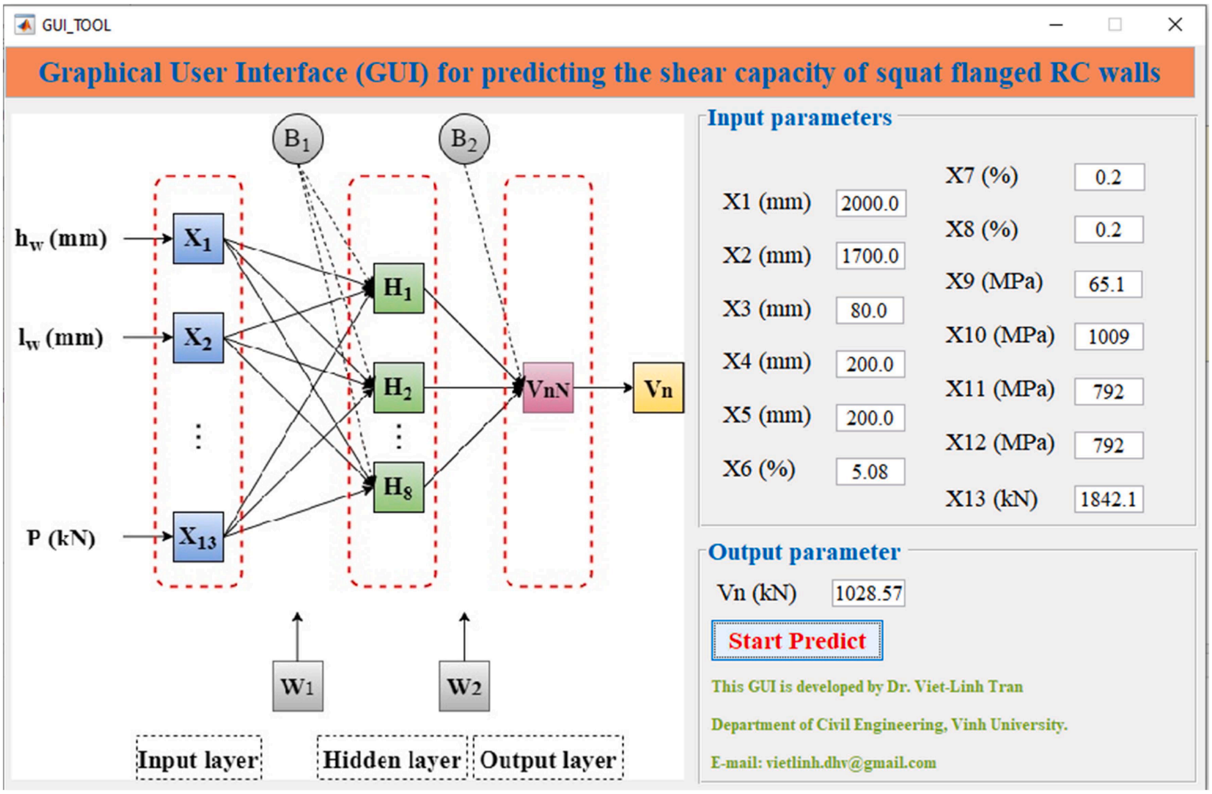

Fig. 18. Practical GUI tool for predicting shear strength of squat flanged RC walls.

and the horizontal reinforcement ratio of the web have a trivial influence on the strength of the walls.

- A practical formula, based on the ANN model, considering thirteen input parameters was proposed to calculate shear strength of squat flanged RC walls.
- A beneficial GUI tool was developed and readily applied for facilitating the design process of squat flanged RC walls.

Declaration of Competing Interest

The authors declare that they have no known competing financial interests or personal relationships that could have appeared to influence the work reported in this paper.

Acknowledgement

This study is supported by the Korea Institute of Energy Technology Evaluation and Planning (KETEP) and the Ministry of Trade, Industry & Energy (MOTIE) of the Republic of Korea (No. 20171510101960).

References

[1] Gulec CK, Whittaker AS, Stojadinovic B. Shear strength of squat rectangular reinforced concrete walls. ACI Struct J 2008;105:488.
[2] Barda F, Hanson JM, Corley WG. Shear strength of low-rise walls with boundary elements. Special Publ 1977;53:149–202.
[3] Wood SL. Shear strength of low-rise reinforced concrete walls. Struct J 1990;87:99–107.
[4] Sánchez-Alejandre A, Alcocer SM. Shear strength of squat reinforced concrete walls subjected to earthquake loading—trends and models. Eng Struct 2010;32:2466–76.
[5] Gulec CK, Whittaker AS. Empirical equations for peak shear strength of low aspect ratio reinforced concrete walls. ACI Struct J 2011;108.
[6] Kassem W. Shear strength of squat walls: a strut-and-tie model and closed-form design formula. Eng Struct 2015;84:430–8. https://doi.org/10.1016/j.engstruct.2014.11.027.
[7] Adorno-Bonilla CM. Shear strength and displacement capacity of squat reinforced concrete shear walls: UNIVERSITY OF PUERTO RICO MAYAGÜEZ CAMPUS; 2016.
[8] ACI-318-14. Building code requirements for structural concrete (ACI 318-14) and commentary. American Concrete Institute; 2014.
[9] ASCE/SEI-43-05. Seismic design criteria for structures, Systems, and Components in Nuclear Facilities. American Society of Civil Engineers, Reston, Virginia2005.
[10] EC8. Eurocode 8: Design of Structures for Earthquake Resistance - Part 1: General Rules. Seismic Actions and Rules for Buildings. 2004.
[11] J. Ma B. Li Experimental and Analytical Studies on H-Shaped Reinforced Concrete Squat Walls 115 2 2018 10.14359/51701144.
[12] Ma J, Li B. Seismic behavior of L-shaped RC squat walls under various lateral loading directions. J Earthq Eng 2019;23:422–43.
[13] Gulec CK, Whittaker AS, Stojadinovic B. Peak shear strength of squat reinforced concrete walls with boundary barbells or flanges. ACI Struct J 2009;106:368.
[14] Del Carpio RM, Whittaker AS, Gulec CK. Predictive equations for the peak shear strength of low-aspect ratio reinforced concrete walls. J Earthq Eng 2012;16:159–87.
[15] Ma J, Ning C-L, Li B. Peak shear strength of flanged reinforced concrete squat walls. J Struct Eng 2020;146:04020037.
[16] Gao W, Karbasi M, Derakhsh AM, Jalili A. Development of a novel soft-computing framework for the simulation aims: a case study. Eng Comput 2019;35(1):315–22. https://doi.org/10.1007/s00366-018-0601-y.
[17] Ghaboussi J, Garrett Jr J, Wu X. Knowledge-based modeling of material behavior with neural networks. J Eng Mech 1991;117:132–53.
[18] Vanluchene R, Sun R. Neural networks in structural engineering. Comp-Aided Civil Infrastruct Eng 1990;5:207–15.
[19] Flood I, Kartam N. Artificial Neural Networks for Civil Engineers: advanced features and applications. ASCE Publications 1998.
[20] Cao X, Sugiyama Y, Mitsui Y. Application of artificial neural networks to load identification. Comput Struct 1998;69(1):63–78. https://doi.org/10.1016/S0045-7949(98)00085-6.
[21] Naderpour H, Kheyroddin A, Amiri GG. Prediction of FRP-confined compressive strength of concrete using artificial neural networks. Compos Struct 2010;92(12):2817–29. https://doi.org/10.1016/j.compstruct.2010.04.008.
[22] Pham TM, Hadi MNS. Predicting stress and strain of FRP-confined square/rectangular columns using artificial neural networks. J Compos Constr 2014;18(6):04014019. https://doi.org/10.1061/(ASCE)CC.1943-5614.0000477.
[23] Chojaczyk A, Teixeira A, Neves LC, Cardoso J, Soares CG. Review and application of artificial neural networks models in reliability analysis of steel structures. Struct Safety 2015;52:78–89.
[24] Salehi H, Burgueno R. Emerging artificial intelligence methods in structural engineering. Eng Struct 2018;171:170–89.
[25] Tran V-L, Thai D-K, Kim S-E. Application of ANN in predicting ACC of SCFST column. Compos Struct 2019;228:111332. https://doi.org/10.1016/j.compstruct.2019.111332.
[26] Tran V-L, Thai D-K, Kim S-E. A new empirical formula for prediction of the axial compression capacity of CCFT columns. Steel Compos Struct 2019;33:181–94.

[27] Tran V-L, Kim S-E. A practical ANN model for predicting the PSS of two-way reinforced concrete slabs. Eng Comp 2020:1–25.
[28] Tran V-L, Kim S-E. Efficiency of three advanced data-driven models for predicting axial compression capacity of CFDST columns. Thin-Walled Struct 2020;152:106744. https://doi.org/10.1016/j.tws.2020.106744.
[29] Nguyen M-S-T, Thai D-K, Kim S-E. Predicting the axial compressive capacity of circular concrete filled steel tube columns using an artificial neural network. Steel Compos Struct 2020;35:415–37.
[30] Chen X, Fu J, Yao J, Gan J. Prediction of shear strength for squat RC walls using a hybrid ANN–PSO model. Eng Comp 2018;34:367–83.
[31] Moradi MJ, Hariri-Ardebili MA. Developing a library of shear walls database and the neural network based predictive meta-model. Applied Sci. 2019;9:2562.
[32] Mangalathu S, Jang H, Hwang S-H, Jeon J-S. Data-driven machine-learning-based seismic failure mode identification of reinforced concrete shear walls. Eng Struct 2020;208:110331.
[33] Kabeyasawa T, Hiraishi H. Tests and analyses of high-strength reinforced concrete shear walls in Japan. Special Publ 1998;176:281–310.
[34] Sanada Y, Kabeyasawa T. Local force characteristics of reinforced concrete shear wall. 8th US National Conference on Earthquake Engineering2006.
[35] Matsui T, Kabeyasawa T, Koto A, Kuramoto H, Nagashima I. Shaking table test and analysis of reinforced concrete walls. Proc, 13th World Conference on Earthquake Engineering2004.
[36] Maier J, Thürlimann B, editors. Bruchversuche an Stahlbetonscheiben. Basel: Birkhäuser Basel; 1985.
[37] Synge AJ. Ductility of squat shear walls. University of Canterbury Library; 1980.
[38] Palermo D, Vecchio FJ, Solanki H. Behavior of three-dimensional reinforced concrete shear walls. ACI Struct J 2002;99:81–9.
[39] Saito H, Kikuchi R, Kanechika M, Okamoto K. Experimental Study of the Effect of Concrete Strength on Shear Wall Behavior. 1989.
[40] Sato S, Ogata Y, Yoshizaki S, Kanata K, Yamaguchi T, Nakayama T, et al. Behavior of Shear Wall Using Various Yield Strength of Rebar Part 1. An Experimental Study 1989.
[41] Seki M, Kobayashi J, Shibata A, Kubo T, Taira T, Akino K. Restoring force verification test on RC shear wall. 1995.
[42] Dabbagh H. Strength and ductility of high-strength concrete shear walls under reversed cyclic loading. University of New South Wales; 2005.
[43] Endo T, Adachi H, Nakanishi M. Force-Deformation Hysteresis Curves of Reinforced Concrete Shear Walls. Proc of the 7th WCEE1980.
[44] NUPEC. NUPEC's Seismic Ultimate Dynamic Response Test, Comparison Report. OECD/NEA/CSNI, Issy-Les-Moulineaux, France, Report No. OCDE/GD (96) 188 …; 1991.
[45] Chiba O, Fukuzawa R, Hatori T, Yagishita K, Sato Y, Higashiura A et al. Experimental study on heavily reinforced concrete shear walls. 1985.
[46] Fukuzawa R, Chiba O, Hatori T, Yagishita K, Watabe M. Study on load-deflection characteristics of heavily reinforced concrete shear walls. Proceedings 1988. p. 4.
[47] Park H-G, Baek J-W, Lee J-H, Shin H-M. Cyclic Loading Tests for Shear Strength of Low-Rise Reinforced Concrete Walls with Grade 550 MPa Bars. ACI Struct. J. 2015; 112.
[48] Li B, Pan Z, Xiang W. Experimental evaluation of seismic performance of squat RC structural walls with limited ductility reinforcing details. J Earthq Eng 2015;19:313–31.
[49] Fu J, Yao J, Cui J, Chen X. Experimental studies and finite element analysis on seismic shear behavior of high-strength rebars shear walls with flanges. China Civ Eng J 2018;51:44–51.
[50] Jiang H, Wang B, Lu X. Experimental study on damage behavior of reinforced concrete shear walls subjected to cyclic loads. J Earthq Eng 2013;17:958–71.
[51] Gupta A, Rangan BV. High-strength concrete (HSC) structural walls. Struct J 1998;95:194–204.
[52] Mansur M, Balendra T, H'ng S. Tests on reinforced concrete low-rise shear walls under cyclic loading. Concrete Shear. Earthquake 1992;95.
[53] Teng S, Chandra J. Cyclic Shear Behavior of High Strength Concrete Structural Walls: Petra Christian University; 2016.
[54] Liu X, Burgueño R, Egleston E, Hines E. Inelastic Web Crushing Performance Limits of High-Strength-Concrete Structural Wall–Single wall Test Program. Report No CEE-RR-2009/03, Michigan State University, 281pp; 2009.
[55] Chiou Y, Mo Y, Hsiao F, Liou Y, Sheu M. Behavior of High Seismic Performance Walls. 13th World Conference on Earthquake Engineering, Vancouver, Canada, August, paper2004.
[56] Nakamura N, Tsunashima N, Nakano T, Tachibana E. Analytical study on energy consumption and damage to cylindrical and I-shaped reinforced concrete shear walls subjected to cyclic loading. Eng Struct 2009;31:999–1009.
[57] Akita T, Kuramoto H, Matsui T, and , Kabeyasawa T. Hysteresis Modeling of RC Shear Walls Based on Static Loading Test. The Eighth US National Conference on Earthquake Engineering. San Francisco, CA, USA.2006.
[58] Maier J. Shear Wall Tests. International Workshop on Concrete Shear in Earthquake. Department of Civil and Environmental Engineering, University of Houston, Houston, TX, USA.1991.
[59] Barda F. Shear Strength of Low-Rise Walls with Boundary Elements. Bethlehem, PA, USA: Lehigh University; 1972.
[60] Han X, Lin J, Wei Y, Xie S. Experimental study on deformation index limits of I-shaped shear walls. China Civ Eng J 2018;51:26–36.
[61] Xiang-Dong G. Framed Shear Walls under Cyclic Loading: University of Houston, Houston. TX: USA; 1999.
[62] Mo Y, Chan J. Behavior of reinforced-concrete-framed shear walls. Nucl Eng Des 1996;166:55–68.
[63] Chaabene WB, Flah M, Nehdi ML. Machine learning prediction of mechanical properties of concrete: Critical review. Constr Build Mater 2020;260:119889.
[64] Fausett LV. Fundamentals of neural networks: architectures, algorithms and applications. Pearson Education India; 2006.
[65] Nikbin IM, Rahimi S, Allahyari H. A new empirical formula for prediction of fracture energy of concrete based on the artificial neural network. Eng Fract Mech 2017;186:466–82.
[66] Hadi Muhammad NS. Neural networks applications in concrete structures. Comput Struct 2003;81(6):373–81. https://doi.org/10.1016/S0045-7949(02)00451-0.
[67] Mathworks I. MATLAB and statistics toolbox release 2012b. Natick (Massachusetts, United States)2012.
[68] Asteris Panagiotis G, Mokos Vaseilios G. Concrete compressive strength using artificial neural networks. Neural Comput Applic 2020;32(15):11807–26. https://doi.org/10.1007/s00521-019-04663-2.
[69] Armaghani Danial J, Hatzigeorgiou George D, Karamani Chrysoula, Skentou Athanasia, Zoumpoulaki Ioanna, Asteris Panagiotis G. Soft computing-based techniques for concrete beams shear strength. Procedia Struct Integrity 2019;17:924–33. https://doi.org/10.1016/j.prostr.2019.08.123.
[70] J.-W. Baek H.-G. Park J.-H. Lee C.-J. Bang Cyclic loading test for walls of aspect ratio 1.0 and 0.5 with grade 550 MPa (80 ksi) shear reinforcing bars ACI Struct. J. 2017;114:969.